Published in final edited form as:
Nat Struct Mol Biol. 2017 May ; 24(5): 475–483. doi:10.1038/nsmb.3400.

Parkin-phosphoubiquitin complex reveals a cryptic ubiquitin binding site required for RBR ligase activity

Atul Kumar[1], **Viduth K Chaugule**[1], **Tara E C Condos**[2], **Kathryn R Barber**[2], **Clare Johnson**[1], **Rachel Toth**[1], **Ramasubramanian Sundaramoorthy**[3], **Axel Knebel**[1], **Gary S Shaw**[2], and **Helen Walden**[1,*]

[1]MRC Protein Phosphorylation and Ubiquitylation Unit, College of Life Sciences University of Dundee, Dundee, UK

[2]Department of Biochemistry, Schulich School of Medicine and Dentistry, University of Western Ontario, London, ON, Canada

[3]Centre for Gene Regulation and Expression, College of Life Sciences, University of Dundee, Dundee, UK

Abstract

RING-BETWEENRING-RING (RBR) E3 ligases are a class of ubiquitin ligases distinct from RING or HECT E3 ligases. An important RBR is Parkin, mutations in which lead to early onset hereditary Parkinsonism. Parkin and other RBRs share a catalytic RBR module, but are usually autoinhibited and activated via distinct mechanisms. Recent insights into Parkin regulation predict large, unknown conformational changes during activation of Parkin. However, current data on active RBRs are in the absence of regulatory domains. Therefore, how individual RBRs are activated, and whether they share a common mechanism remains unclear. We now report the crystal structure of a human Parkin-phosphoubiquitin complex, which shows that phosphoubiquitin binding induces a movement in the IBR domain to reveal a cryptic ubiquitin binding site. Mutation of this site negatively impacts on Parkin's activity. Furthermore, ubiquitin binding promotes cooperation between Parkin molecules, suggesting a role for interdomain association in RBR ligase mechanism.

*Corresponding author. Tel: +44 1382 384109; h.walden@dundee.ac.uk.

Author contributions

AK designed and performed experiments, solved the crystal structures, analysed data and wrote the manuscript. VKC purified Miro1, made labelled ubiquitin and developed the labelled ubiquitin based assay, and performed the RING2(Rcat) loading experiments. TEC performed the NMR CSP experiments, KRB did the AUC experiments. RT cloned several constructs. CJ, RS and AK purified various reagents for assays. GSS and HW designed the experiments, analysed data and wrote the manuscript.

Conflict of interest

I declare that the authors have no competing interests as defined by Springer Nature, or other interests that might be perceived to influence the results and/or discussion reported in this paper.

Accession codes

The protein structure files reported in this manuscript are available from the Protein Data Bank with accession codes 5N2W, and 5N38.

Data availability statement

All constructs are available on request from the MRC Protein Phosphorylation and Ubiquitylation Unit reagents Web page (http://mrcppureagents.dundee.ac.uk). All other data are available from corresponding author upon reasonable request.

Europe PMC Funders Author Manuscripts

Introduction

Parkinson's Disease (PD) is a neurodegenerative disorder characterised by the progressive loss of dopaminergic neurons, bradykinesia and tremor 1. Although primarily a sporadic disorder, mutations in several genes are associated with different Parkinsonism syndromes 2, including the genes *PARK2* and *PARK6* which lead to autosomal recessive juvenile Parkinsonism (ARJP) 3,4. *PARK2* and *PARK6* encode Parkin E3 Ubiquitin ligase and PTEN-induced kinase (PINK-1), respectively, and maintain mitochondrial homeostasis 5–8. In addition to its role in mitochondrial protein control, Parkin also regulates protein degradation and induces aggresome formation by K63-linked ubiquitination 9–11.

Parkin belongs to the RBR E3 ubiquitin ligase family, characterised by a RING domain (RING1) followed by an 'in-between RING' (IBR) domain and a catalytic domain (RING2 or Rcat 12). RING1 is structurally similar to canonical RING-type E3 ligases, and shares the function of binding to E2 ubiquitin conjugating enzymes. In contrast, RING2(Rcat) adopts a linear zinc-binding fold 13,14 and possesses a catalytic cysteine capable of forming a thioester bond with activated ubiquitin 13,15–19. The linking 'IBR' domain adopts the same fold as the RING2(Rcat) 20, however its functional role remains unclear. RBR ligases contain additional domains outwith the RBR module. Parkin has an N-terminal ubiquitin-like domain (UBL), which shares 65% homology with ubiquitin, and a zinc-binding RING0 or unique parkin domain (UPD) 21. Parkin adopts an autoinhibited conformation mediated by multiple domain-domain interactions 22–26. This autoinhibition is released by PINK1-dependent phosphorylation of ubiquitin and the UBL domain of Parkin, leading to activation of Parkin 27–32. Additional RBR ligase family members include HOIP, which is a subunit of the linear ubiquitin chain assembly complex (LUBAC) 33, and the human homologue of Ariadne, HHARI 34. The catalytic activity of HOIP is also regulated through autoinhibition, mediated by its UBA domain, which interacts with the other subunits of LUBAC, HOIL-1L and SHARPIN to activate HOIP 17,33,35,36. HHARI is also autoinhibited, mediated through its Ariadne domain 37. HHARI activation requires interaction of the UBA domain of HHARI with NEDD8 38,39. Thus our current understanding of Parkin and other RBRs suggests distinct modes of regulation. In the case of Parkin, we and others have shown that the binding of phosphoubiquitin, leads to Parkin activation via removal of the inhibitory effect of the Ubl domain 23,24,40–43. However, all the structural insights into Parkin are in the context of the autoinhibited state 23–25, or in the absence of the regulatory Ubl domain 16,25,26,43. Insights into HHARI are also based on an inactive conformation 37. Recent insights into the catalytic mechanism of the RBR family have come from structural and physical analyses of HOIP 14,44. The crystal structure of the catalytic RING2-Like (RING2L) or Rcat domain of HOIP in complex with ubiquitin revealed how linear chains are assembled 14, while a recent complex of the RBR module of HOIP in complex with a charged E2~ubiquitin conjugate revealed a series of allosteric ubiquitin-binding sites coupled to a swapped dimer of the RING2L(Rcat) domain between RBR molecules44. Furthermore, the RING2(Rcat) of HHARI has a ubiquitin binding site important for E2~ubiquitin recruitment 45, and the RING1 of HHARI supports an open conformation of the E2~ubiquitin conjugate. In contrast a structure of the RING0-RBR (R0RBR) domains from *Pediculus humanus corporis* Parkin, in complex with phosphoubiquitin does not show

domain swapping between RBR modules, but rather revealed a conformational change in the IBR domain upon phosphoubiquitin binding 43. Our current understanding is derived from snapshots of individual domains of large multidomain complexes. However, how RBR ligases function in the context of their regulatory domains remains unclear, and whether they share a universal catalytic mechanism remains unclear.

We report here the crystal structures of activated human Parkin (UblR0RBR), and a phosphomimic Parkin (S65DUblR0RBR), in complex with phosphoubiquitin, at 2.7 and 2.6 Å resolution respectively. All Parkin domains are present, and in contrast to earlier predictions of large conformational rearrangements upon activation, the Parkin structures reveal subtle, local changes that result in a series of cryptic ubiquitin or ubiquitin-like binding regions that are essential for Parkin function. We find an essential role of the IBR domain in ubiquitin recruitment and Parkin activity. Furthermore, comparative analyses with the HOIP and HHARI modules reveals common ubiquitin or ubiquitin-like binding sites. In particular, comparison with the RBR of HOIP suggests a potential unifying mechanism of cooperation between multiple RBR modules in the mechanism of ubiquitin ligase activity.

Results

Crystal structure of UBLR0RBR Parkin in complex with pUb reveals activated state of Parkin

Previous studies by ourselves and others suggest that binding of phosphoubiquitin to Parkin relieves the autoinhibition by the UBL domain. Consistent with this, the UBL domain displays weaker binding to the R0RBR fragment of Parkin in *trans* upon phosphoubiquitin binding 23,24,40–43,46. In order to understand the allosteric regulation by phosphoubiquitin, we crystallised a complex of Parkin UBLR0RBR (Δ84-143) with a phosphoubiquitin (pUb) suicide probe (pUb3BR, pUb bromopropylamine). To enable the formation of stable, well diffracting crystals, we generated a covalent Parkin-pUb complex by ligating the pUb3BR probe to a cysteine residue on the surface of Parkin. The cysteine was provided by mutating Gln347, as described previously 43. The structure of activated Parkin was refined to 2.7 Å (Table 1), with good geometry and refinement statistics. The crystal structure of the Parkin-pUb complex reveals the activated state of Parkin, containing all 5 domains of Parkin UBL, RING0, RING1-IBR-RING2(Rcat) and pUb (Fig 1a). In the asymmetric unit, UBL, RING1-IBR-RING2(Rcat) are contributed from one molecule whereas RING0 and pUb are from another molecule, with the biological unit via symmetry related molecules (Supp Fig 1a). Comparison of the activated state of Parkin-pUb with the apo, inactive UBLR0RBR structure 23 shows that although some small rearrangements occur, the UBL-RING1 interface, primarily formed by between β3 and β5 of the UBL domain, and helix H1 of the RING1 domain, remains largely intact in the presence of phosphoubiquitin (Fig 1b). The largest structural rearrangement upon activation is the movement of the IBR domain. Helix H3 of the RING1 domain straightens, leading to global movement of the IBR domain (henceforth this helix is referred to as H3-IBR), and creating a void between the UBL and IBR domains. This straightening of the H3-IBR helix is also observed in the insect Parkin R0RBR complex with pUb that lacks the UBL domain 43. In the apo structure this UBL-IBR interface is formed primarily through interactions of His11

of the UBL domain with Lys369, Glu370 of the IBR domain, and surrounding residues, and these interactions are lost in the phosphoubiquitin-bound complex. Phosphorylation of the UBL domain by PINK-1 has been shown to weaken association of the UBL domain with R0RBR Parkin 23,24,42,46,47. Therefore, we wondered whether inclusion of a negative charge at Ser65 to mimic phosphorylation would lead to displacement of the UBL domain in presence of pUb. To test this, we crystallised a covalent complex of S65D-UBLR0RBR Parkin with the pUb suicide probe. In this structure, refined to 2.6 Å resolution, the S65D-UBL domain remains associated with RING1 (Supp Fig.1b). However, there are local conformational rearrangements between UBLR0RBR/S65SD-UBLR0RBR in complex with pUb and the apo structure of UBLR0RBR. In the apo structure of UBLR0RBR, residues 383-390, part of the tether that connects the IBR domain to the Repressor Element of Parkin (REP) are disordered 23,25. In contrast, this tether, residues 387-390, is ordered and traceable in the WT Parkin-pUb complex, with Arg392 pointing towards the disordered side-chain of Lys48 in the UBL domain. This Arg392-Lys48 creates an electrostatic repulsion, while Gln389 and Tyr391 cement the association of the UBL-RING1 interface, resulting in flexibility of the 62-65 loop in the UBL domain (Supp Fig 1b). Upon inclusion of a negative charge at position 65, Tyr391 relocates from the UBL-RING1 interface, resulting in disorder of the IBR-REP tether and ordering of the 62-65 loop in the UBL domain (Supp Fig 1c). We wondered whether mutation of these residues would enable the UBL domain to bind ΔUBL-Parkin in the presence of pUb. In the absence of pUb, the UBL domain associates with ΔUBL-Parkin (80-465) with a dissociation constant (Kd) in the low micromolar range 22–24,43 (Supp Fig 1d). The presence of pUb blocks the UBL interaction with ΔUBL- Parkin (Supp Fig 1d). Gln389Ala, Tyr391Ala and Arg392Ala mutation in ΔUBL-Parkin does not permit UBL re-association in the presence of pUb (Supp Fig 1d). Given that the structures clearly show the UBL-RING1 interface persists in the presence of pUb, we wondered whether the loss of association in solution could be due to a weakened UBL-IBR interface (Fig 1B), rather than UBL-RING1 interface. To test this, we expressed and purified human Parkin lacking the IBR domain, and measured the interaction of the UBL domain with Parkin, using isothermal titration calorimetry (ITC). The UBL domain does not associate with ΔUBL-ΔIBR (80-329,383-465) (Fig 1c). In order to understand the role of the IBR domain we assayed this mutant for E3 ligase activity. ΔUBL-Parkin is active, both in the absence and presence of phosphoubiquitin (Fig 1d). In contrast, deletion of the IBR domain in ΔUBL-Parkin leads to complete loss of Parkin activity, which cannot be rescued by the addition of pUb. It is a possibility that removal of the IBR domain results in a constrained version of Parkin that lacks the flexibility needed for maintenance of its catalytic domains. In order to rule this possibility out, we purified ΔUBL-ΔIBR containing a 10-residue (Gly-Thr-Ser-Gly-Thr-Ser-Gly-Ser-Ala-Ser) (ΔUBL-ΔIBRxL10) linker to span the 28 Å distance required, and assayed for ubiquitination activity (Fig 1d). These constructs lacking the IBR domain are folded, monodisperse and migrate at the expected molecular weight, consistent with folded proteins. In contrast to wild-type and ΔUBL-Parkin, both ΔUBL-ΔIBR and ΔUBL-ΔIBRxL10 Parkin lack ubiquitination activity, even in the presence of phosphoubiquitin. Interestingly, the surface of the UBL domain when phosphorylated would result in repulsion with the negatively charged surface of IBR, supporting a weakened UBL-IBR interaction (Supp Fig 1e). The observation that the UBL domain and pUb both interact with IBR, on opposite sides, could explain the competitive mode of binding to Parkin that

has previously been observed 23,24. Taken together, these results show that activation of Parkin by phosphoubiquitin binding involves loosening of the UBL-IBR interface, caused by a straightening of the H3-IBR helix. Furthermore, these experiments show that the association of the UBL domain with the rest of Parkin depends upon the presence of the IBR domain in addition to the more extensive RING1 surface, and that Parkin activity requires an intact IBR domain.

Parkin activation exposes ubiquitin or ubiquitin-like binding surfaces that are essential for Parkin activity

The straightening of the H3-IBR helix caused by phosphoubiquitin binding results in a void being created between the UBL and IBR domains (Supp Fig 2a). Intriguingly, analysis of the crystal packing of activated Parkin reveals that this void is occupied by the UBL domain of another molecule of Parkin (Supp Fig 2b). The UBL domain of Parkin shares 65% sequence similarity with ubiquitin. We therefore wondered whether the void created by the loosening of the UBL-IBR interaction, occupied in our crystal structures by the UBL domain of a second molecule of Parkin, could accommodate ubiquitin. To explore this idea, we modelled ubiquitin into the void (Fig 2a). This arrangement reveals potential surfaces on Parkin that could interact with ubiquitin, referred to as Ubiquitin Binding Region (UBR) 1,2, and 3, respectively (Fig 2). UBR1 is contributed by the UBL domain of Parkin, mediated by His11, Phe13, Arg33, Gln34 (Fig 2b). Mutation of UBR1 residues on Parkin results in a minor reduction in ubiquitin chain formation, but no observable decrease in substrate ubiquitination, in this case Miro1 (Fig 2b). UBR2 and UBR3 are formed on the straightened helix (H3) of RING1 and the IBR of Parkin, respectively. The potential ubiquitin binding surfaces are mediated by Arg275, Gln317, Tyr318, Glu321 on H3 of RING1, and Arg334 and Pro335 of the β-hairpin on IBR (Fig 2c). Mutations in UBR2 (R275A, Y318A, E321A) and UBR3 (R334A) result in loss of E3 ligase activity, both in ubiquitin chain formation and Miro1 ubiquitination (Fig 2c). Therefore, UBR2 and UBR3, but not UBR1, are important for Parkin activity. In order to further clarify which regions of activated Parkin interact with ubiquitin, we performed NMR chemical shift perturbation experiments of the R0RBR fragment of Parkin in complex with pUb (Fig 2d). Upon addition of unlabelled Ub to the R0RBR-pUb complex it was clear that the IBR domain was a major site of interaction. The largest chemical shift changes occur for residues G329-R334 of the β-hairpin and the adjoining loop (G361-A363, R366) of the IBR domain. Changes were also observed in the straightened helix (H3) of RING (R314, V324) near those observed in the crystal structure. However, several of these resonances are broadened by pUb binding and are therefore difficult to visualise in the NMR spectra. Nevertheless, this analysis shows a large ubiquitin interaction surface in activated Parkin that is consistent with that for UBR2 and UBR3 sites predicted from the crystal packing analyses. These findings suggest a role for ubiquitin (or ubiquitin-like protein) binding at surfaces exposed upon pUb binding in the regulation of Parkin activity. Consistent with this, a recent study shows that modification of the IBR domain at Lys349 and Lys369 by the ubiquitin-like protein ISG15, positively regulates Parkin activity 48. Interestingly, Lys349 is also a target of Parkin autoubiquitination activity 13. Therefore, we wondered whether Parkin modification by ubiquitin can influence Parkin activity. To explore this possibility, we generated a covalently linked Parkin carrying a ubiquitin chain (UBLR0RBR347Cys~pUb-M1-$(UBS65A)_3$, to mimic polyubiquitinated

Parkin. In comparison with UBLR0RBR347Cys~pUb or providing pUb to UBLR0RBR in *trans*, UBLR0RBR347Cys~pUb-M1-$(UBS65A)_3$ activity is dramatically enhanced (Supp Fig 2c). Taken together, these data suggest an important role for the displacement of the UBL-IBR interface, revealing that modification of the IBR, phosphorylation of Ser65 in the UBL-IBR interface, and pUb binding to the IBR domain all contribute to the creation of a ubiquitin/ubl binding region, and that ubiquitin binding stimulates Parkin activity.

The UBL-IBR ubiquitin binding site recruits the donor ubiquitin

The arrangement of phosphoubiquitin of one molecule of Parkin, and the UBL domain of a second molecule, is reminiscent of the activator ubiquitin and donor ubiquitin recently described in the structure of the RBR of HOIP in complex with a charged E2 44 (Fig 3a). Furthermore, UbcH7 interaction with phosphorylated Parkin is enhanced 20 fold by the addition of phosphoubiquitin and charging of the E2 with ubiquitin 23,49. Thus we wondered whether the ubiquitin binding site created from the activation of Parkin by phosphoubiquitin could accommodate the charged E2~ubiquitin conjugate. To test this, we measured UbcH7 or UbcH7~ubiquitin interaction with phosphoparkin (pParkin) or a UBR2 mutant pParkinE321A, in the presence of pUb. ITC experiments show a similar affinity of pParkin or pParkinE321A for UbcH7 (Kd of 19 and 23.5 μM respectively) in the presence of pUb, suggesting that mutation of the ubiquitin binding region of Parkin does not interfere with E2 binding (Fig 3b). In contrast, while phosphoParkin binds to UbcH7~ubiquitin with a 30-fold higher affinity, this enhanced binding is diminished for phosphoParkinE321A (~2.5 fold) (Fig 3b). In addition, size exclusion chromatography of these complexes reveals that mutation of E321 to alanine abolishes formation of the phosphoParkin UbcH7~Ub complex in the presence of phosphoubiquitin (Supp Fig 3a). We ruled out the possibility that mutation of E321 leads to loss of phosphoubiquitin binding by ITC measurement (Supp Fig 3b). These data suggest that the ubiquitin carried by charged E2 binds at the UBR regions in activated Parkin. Previous studies have shown that when the only source of ubiquitin is phosphoubiquitin, Parkin cannot catalyse ubiquitin chains 49,50. However, UbcH7 can be charged with pUb 50. Furthermore, measurements of Parkin fragments interacting with either ubiquitin or pUb showed a similar isotherm profile, but with much tighter binding to pUb 23. Both these observations suggest that the pUb-binding pocket on the surface of Parkin is the dominant ubiquitin binding site. Therefore we wondered whether loading of E2 with pUb redirects the conjugate to the pUb binding site on the Parkin, rather than going to the donor ubiquitin binding site. To test this, we “activated” Parkin using either pUb, or UbcH7 charged with pUb (Ubch7~pUb). Interestingly, UbcH7~pUb, but not UbcH7~ubiquitin, activates Parkin to a similar extent as pUb alone (Fig 3c). Taken together, these data suggest that the cryptic ubiquitin binding site created between the UBL-IBR domains upon Parkin activation, recruits the donor ubiquitin as carried by the E2.

Cooperation between multiple Parkin molecules promotes ubiquitin transfer

Using the position of the UBL domain, the HOIP RBR/E2~Ub structure, and the chemical shift perturbations on Parkin as guides, we modelled an activated Parkin-donor ubiquitin complex (Supp Fig 4a). In the model, with only one molecule of Parkin, it is difficult to envision how the E2 of the E2~Ub conjugate would reach the proposed E2 binding site at the base of the RING1. In addition, it is difficult to determine how the ubiquitin would reach

the catalytic cysteine in the RING2(Rcat). Indeed, despite many efforts to understand how the catalytic cysteine in the RING2(Rcat) domain mechanistically directs Parkin activity, previous Parkin structures show that the Cys431 of the RING2(Rcat) domain is ~35 Å away (using the sulfur of Cys431, and the side-chain oxygen of Thr240 as the reference points) from the predicted E2 binding site on RING1 25. Furthermore, multiple groups have reported that Cys431 is occluded by RING0 16,25,26. In our crystal structure of the Parkin-pUb complex, one molecule of activated Parkin accommodates a UBL domain from a neighbouring molecule, which we model as donor ubiquitin. This modelled donor ubiquitin packs against the catalytic RING2(Rcat) domain of a neighbouring Parkin molecule (Fig 4a). This quarternary arrangement of Parkin molecules can also accommodate an E2, with proposed interactions with the RING1 and REP of molecule 2, satisfying observed E2 interaction sites in HOIP and HHARI 44,45 (Fig 4a). Therefore, we wondered whether the UBR2 donor ubiquitin binding site would affect the loading on ubiquitin onto the catalytic cysteine (C431). In order to test this, we designed an *in vitro* assay that evaluates the transfer of donor ubiquitin from the E2 to the RBR catalytic residue. First, we generated a Parkin RING2(Rcat) mutant, able to trap the catalytic Parkin~Ub intermediate 13,17, referred to as R0RBR^{CH}. This species has a serine in place of the catalytic cysteine (C431S) and a His433Ala mutation in order to trap an ester-bound ubiquitin and impede any subsequent discharge. This R0RBR^{CH} Parkin species can be charged with ubiquitin and was sensitive to sodium hydroxide hydrolysis thus confirming the RING2(Rcat)-ubiquitin ester link. The addition of phosphoubiquitin in this setup greatly enhances the RING2(Rcat) charging by around 7-fold while a catalytic Cys431Ala mutant (R0RBR C431A) Parkin cannot be charged with ubiquitin in either scenario (Fig 4b). We then generated a UBR2 patch mutant of Parkin in this background, R0RBR^{CH} E321A. In contrast to R0RBR^{CH}, this mutant is defected in ubiquitin charging even in the presence of phosphoubiquitin (26-fold less). Finally, a combined mutant of the phosphoubiquitin patch and the UBR2 patch (R0RBR^{CH} H302A+E321A) was drastically reduced (60-fold less) in ubiquitin charging of the RING2(Rcat) (Fig 4b). Recent studies have suggested a physiological role for self-association of Parkin molecules. For example, in 2013, two independent studies reported the observation that catalytically compromised Parkin (C431 mutants) could not translocate to the mitochondria after PINK1 activation 15,19. However, co-expression of C431 mutant Parkin with either wild-type Parkin, or other mutations including the R275W that would affect the UBR2 binding site, could rescue this translocation defect. These observations raise the possibility of cooperation between Parkin molecules. We have demonstrated that mutation of the donor ubiquitin binding site UBR2 in Parkin results in loss of Miro1 ubiquitination (Fig 2c). Thus we wondered whether a constitutively phosphoubiquitin-bound form of Parkin could support the activity of otherwise inactive Parkin, in this case phosphoParkinE321A. To test this, we took the crystallised species of Parkin UblR0RBR covalently linked to phosphoubiquitin, and titrated it into phosphoParkinE321A (Fig 4c). We find that wild-type phosphoParkin can ubiquitinate Miro1 (Fig 4c). In contrast, phosphoParkinE321A is defective in Miro1 ubiquitination (Fig 4c). Addition of autoinhibited UblR0RBR does not significantly enhance Miro1 ubiquitination (Fig 4c, Supp Fig 4b). However, addition of equimolar amounts of active UblR0RBR complexed with pUb rescues Miro1 ubiquitination to a greater extent than having the UblR0RBR.pUb complex alone (Fig 4c). These data suggest that the activity of inactive Parkin molecules can be

stimulated by the presence of activated Parkin molecules. Taken together, these data demonstrate that Parkin molecules can function together to ligate ubiquitin.

Discussion

Previous extensive characterisation of Parkin has shown that Parkin exists in an autoinhibited state, mediated through multiple domain-domain interactions, including the UBL-RING1 interface, the REP blocking the proposed E2 binding site, and the proposed occlusion of the catalytic cysteine, Cys431, by the RING0 domain 16,22–26. All these inhibitory mechanisms are relieved by the activation of Parkin by pUb 27,28,30. pUb and the phosphorylated UBL domain are unable to simultaneously bind to R0RBR Parkin in solution, *in trans*, suggesting an allosteric regulation of Parkin by pUb binding 23,24,42,46. In addition, previous studies have led to predictions of large conformational changes in Parkin upon activation. Interestingly, a computational analysis of Parkin suggest that phosphorylation of the UBL domain initiates a large change, mediated by the 65 amino acid linker between the UBL domain and RING0 (residues 77-140) 47. An important caveat of our current understanding of the mechanism of Parkin activity is that structures are either of fragments of Parkin (R0RBR) 16,25,26, or all domains but lacking the UBL-RING0 linker 23,24. However, in a low resolution structure of full length rat Parkin, the linker is present in the protein, but is completely disordered in the crystal and can't be modelled 25. The UBL domain and R0RBR domains remain as they are in the absence of the linker 23,24. Interestingly, while the linker length, although not the composition, is conserved down to *Drosophila* 23,24, Parkin from nematodes does not have a long linker between the UBL and RING0 domains, therefore the functional importance of this linker is still unclear. In this study, we present a modified model for Parkin regulation, based on the first structures of an RBR ligase in the activated state, complete with regulatory domains. Our structures reveal that in contrast to the large conformational changes that have been predicted for Parkin function, activation of Parkin results in local rearrangements of Parkin domains to reveal ubiquitin binding sites. These ubiquitin binding sites recruit molecules of ubiquitin, or ubiquitin carried by an E2, to bridge Parkin molecules and allow the utilisation of catalytic domains from neighbouring molecules. In this model, the UBL-IBR interaction (Fig 5a) is perturbed by UBL phosphorylation or pUb binding, displacing the IBR from the UBL domain (Fig 5b/c). This IBR displacement opens a ubiquitin binding pocket on the helix (H3)-IBR surface. A (donor) ubiquitin on loaded E2 occupies this new pocket while E2 occupies the proposed sites on RING1, and the RING2(Rcat) of the neighbouring molecule of Parkin (Fig 5d).

Based on current data, Parkin is unique in the RBR family in that it has a distinct structural arrangement of RING1-IBR-RING2(Rcat) domains, where RING2(Rcat) and RING1 are in juxtaposition. In contrast, in HOIP and HHARI RING2(Rcat) and RING1 are separated by IBR (Supp Fig 5a) 37,44. Although RBRs share a conserved catalytic RING1-IBR-RING2(Rcat) module, they are usually autoinhibited and activated via distinct mechanisms. pUb binding or UBL phosphorylation releases Parkin autoinhibition 27–32, HOIP autoinhibition is released by UBA mediated interactions with LUBAC constituents HOIL-1L or SHARPIN 22,29,30,33,36,38,51 and HHARI autoinhibition is released by NEDD8 binding at the UBA 38. In the structure of full-length HHARI, the proposed NEDD8 binding

Europe PMC Funders Author Manuscripts

pocket (Supp Fig 5b) corresponds to the pocket is occupied by pUb or allosteric ubiquitin (Ub_{allo}) in active Parkin or HOIP, respectively. This suggests that NEDD8 binding to HHARI would have a similar effect as pUb or Ub_{allo} binding has on Parkin and HOIP. Inactive HHARI and Parkin have a compact H3-IBR region (Supp Fig 5c). Active Parkin and HOIP structures enable pUb or Ub_{allo} binding on one side of the H3-IBR region which in the case of Parkin is occluded when inactive, and allows donor ubiquitin binding on the opposite side of the H3-IBR (Supp Fig 5d). Therefore, we speculate that blocking the donor ubiquitin binding site on one side of the H3-IBR, relieved upon pUb or Ub_{allo} binding on the opposite side via opening of the H3-IBR to allow donor ubiquitin binding, could be a common mechanism of regulation in RBR ligases.

The structure of HOIP-RBR in complex with loaded E2 also suggests that the RING1 and RING2(Rcat) of the same molecule cannot crosstalk as they are not close enough to allow catalysis of thioester formation, mediated by the catalytic cysteines of E2 and RING2(Rcat) (Supp Fig 5e). In the active state of HOIP-RBR the processive unit is formed by the RING2(Rcat) of molecule 1, and the RING1-IBR of a second molecule, where E2 interacts with the RING2(Rcat) of molecule 1 and RING1 of molecule 2 whereas the donor ubiquitin interacts with the RING2(Rcat) of molecule1 and the H3-IBR of molecule 2 (Supp Fig 5e). In contrast, in Parkin the processive unit is formed by RING1-RING2(Rcat) of molecule 1, and the IBR of molecule 2 (Fig 4d). This difference in the arrangement of domains between Parkin and HOIP, in the active state, is consistent with the differences in RING1-IBR-RING2(Rcat) structural organisation in three dimensions (Supp Fig 5a). Interestingly, inter/intra-molecular pairing of RING1-RING2(Rcat)-IBR domains of RBRs with E2 and donor ubiquitin explains the previous observations that Parkin and other RBRs favour the extended ‘open’ conformation of loaded E2 44,45. Furthermore, a role for Parkin oligomerisation or self-association has previously been reported 15, along with reports of Parkin having ubiquitin-binding activity 19,22. Our structures of active Parkin support the idea that PINK1 induces structural changes in Parkin that stimulate ubiquitin binding. In the context of the mitochondrial membrane environment, where Parkin functions in mitophagy 52), high local concentrations of Parkin, recruited by PINK1-catalysed phosphorylation of ubiquitin, could result in the feed-forward amplification of Parkin-mediated ubiquitination observed at the mitochondria 52,53. Furthermore, it has been reported that Parkin functions with the linear chain assembly complex, LUBAC, comprising two RBR proteins in HOIP and HOIL-1L 54. The structures reported here open up the possibility of cooperation between RBR modules, and therefore we speculate that there is a possibility that RBR ligases can function in concert.

Within the RBR module, it has long been predicted that RING1 recruits the E2 55, recently formally demonstrated for HHARI and HOIP 44,45; and that the RING2(Rcat) domain, harbouring the catalytic cysteine, is the catalytic intermediate domain 18. However, a functional role for the IBR domain has been less clear. Our observation that covalent modification in the IBR enhances Parkin activity, and that deletion of IBR or mutations in IBR leads to loss of Parkin activity, coupled with a recent report of increased Parkin activity after ISG15ylation on K349 and K363 of the IBR 48, suggest a crucial role for the IBR in Parkin function. Our study suggests that the role of the IBR, together with H3 (helix connecting RING1 and IBR), is to mediate interactions with the inhibitory UBL domain in

the inactive state, and the donor ubiquitin in the active state, respectively. Furthermore, the IBR and RING2(Rcat) of RBRs are structurally similar folds, each containing two β-hairpin turns. Comparison of Parkin and HOIP structures in the active state reveals that the IBR can interact with 2 ubiquitin molecules (pUb or $Ub_{allo,}$ and donor ubiquitin) spanning across both β-hairpins (Supp Fig 5a). Similar to the IBR, the RING2(Rcat) of HOIP also interacts with 2 ubiquitin molecules (donor and acceptor ubiquitin) 14,44 mediated by both β-hairpins (Supp Fig 5f). Interestingly this observation furthers the idea that the ubiquitination process is facilitated by the inherent ability of E1, E2 and E3 proteins to interact with ubiquitin 56. In our Parkin structures, only one ubiquitin binding site is captured, predicted to be the donor ubiquitin binding site, while the acceptor ubiquitin may occupy the opposite surface, in a manner similar to HOIP (Supp Fig 5g); However, we cannot rule out that there may be subtle differences in the acceptor ubiquitin or substrate recognition between RBRs that result in different type of modifications by different RBRs.

Taken together, our data suggest a common mechanism of regulation in RBRs. First, autoinhibition via blocking a donor ubiquitin binding pocket on H3-IBR. Second, release of autoinhibition by a UBL, be that phosphoubiquitin, NEDD8, ISG15, or ubiquitin itself, opening the H3-IBR binding site. Third, donor ubiquitin binding on the H3-IBR accompanied by a bridging of RBR molecules to facilitate access to the catalytic cysteine. Given the importance of Parkin function in mitophagy and PD, understanding the multiple regulatory modes required for function will provide a framework for the design of small molecules to modulate Parkin activity.

Online Methods

Protein expression and purification

UBLR0RBRGln347Cys (resi 1-83, 144-465) and S65DUBLR0RBRgln347Cys (resi 1-83, 144-465) were expressed as His-Smt-3 fusion. FL, various mutants and truncated constructs of Parkin were expressed as His-SUMO fusion. Constructs were expressed in in BL21 (DE3) *E. coli* cells and purified as previously described (21,22). Parkin or ubiquitin were phosphorylated using *Pediculus humanus* PINK1 (126-C) or *Tribolium castaneum* PINK1 (TcPINK1), expressed and purified as previously described 23,57. Miro1 (181-592) and fluorescently labelled ubiquitin (Ub^{IR800}) were prepared as previously described 23.

Preparation of phospho-Ubiquitin-3BR probe

Ubiquitin was expressed as ubiquitin 1-75-Mxe-intein/chitin binding domain using pTXB-1 vector ((DU49003)) in BL21 *E. coli* cells. Cells were induced at 0.5 OD_{600} with 300μM IPTG (Isopropyl β-D-1-thiogalactopyranoside) and incubated at 20°C overnight. Cells were lysed in lysis buffer (20mM Na_2HPO_4 pH7.2, 200mM NaCl and 0.1mM EDTA). Clear lysate was incubated with Chitin resin, after washing with 2-column volume of lysis buffer protein was eluted in 20mM Na_2HPO_4 pH6.0, 200mM NaCl and 0.1mM EDTA and 0.1mM MESNA (Sodium 2-mercaptoethanesulfonate). Eluted material was reacted with 3-Bromo-propyl amine hydrobromide (SIGMA) as described before 58,59. After reaction, protein was purified on size-exclusion column pre-equilibrated with PBS. Fractions containing ubiquitin were collected and phosphorylated using *Pediculus humanus* GST-PINK1, and further

purified by size-exclusion chromatography. M1-(UbS65A) $_3$-pUb-3BR was prepared similarly by expressing M1 linked linear tetra-ubiquitin, in the same vector, with distal ubiquitins' Ser65 mutated to Ala.

Preparation of UBLR0RBR347Cys~pUb/S65DUBLR0RBR347Cys~pUb

We first mutated UBLR0RBR Parkin to contain a cysteine residue at position 347. The corresponding residue in *Pediculus humanus* Parkin is a cysteine, and this enabled R0RBR Parkin to react with the phosphoubiquitin-3BR probe, as described previously 43. UBLR0RBRGln347Cys/S65DUBLR0RBRGln347Cys was reacted with 3 fold molar excess of pUb-3BR probe at room temperature for 2hrs. Complex was purified by size-exclusion chromatography in 20mM Tris pH7.5, 75mM NaCl and 250μM TCEP buffer. UBLR0RBR347Cys~pUb-(M1-UbS65A)$_3$ was prepared using the same method.

Crystallisation and Structure determination

UBLR0RBRGln347Cys/S65DUBLR0RBRGln347Cys~pUb were crystallised at 4°C in sitting drop plates by mixing 1:1 of protein (7mg/ml) and mother liquor (100mM Tris pH 8.5, 200mM TMAO, PEG MME 2000). Crystals were flash frozen in liquid nitrogen using 20% of PEG400 as cryo-protectant in the original mother liquor. Data were collected at Diamond Light Source, wavelength 0.979Å. Data were solved by molecular replacement program Phaser in CCP4 60 by using UBL (1-76), RING0 (142-216), RING1 (229-328), IBR (329-377) and RING2(Rcat) (415-465) domains of apo Parkin structure (5c1z) and pUb (4wzp) as ensembles. Solution obtained by phaser was built and refined in iterative cycles by using coot 61 and autobuster 62, respectively. Ramachandran values were calculated using Molprobity 63. Both structures have excellent geometry with ~95% of residues in the most favoured regions. The structure coordinates and structure factors have been deposited in the Protein Data Bank, with the accession codes 5N2W and 5N38.

Size-exclusion chromatography

Size-exclusion chromatography experiment was performed on analytical column superdex-75, pre-equilibrated with 50mM HEPES pH 7.5, 200mM NaCl, 250μM of TCEP. 10μM of Phospho-Parkin was incubated with 2 fold molar excess of pUb or pUb and UbcH7~Ub for 1 hr prior to loading on column. UbcH7~Ub was prepared as described previously 23.

Isothermal titration calorimetry

ITC experiments were performed using PEAQ-ITC (Malvern instruments), and data were analysed using single-site binding model. 30μM of WT-Phospho-Parkin/Phospho-ParkinGlu321Ala (premixed with 1.2 fold molar excess of pUb) were titrated using 1.6mM or 1.48mM of UbcH7 in the syringe, respectively. 21.4μM of ΔUBL, 40μM of ΔUBL (Gln389Ala, Tyr291Ala, Arg392Ala) premixed with 1.2 fold molar excess of pUb, and 19μM of ΔUBL-ΔIBR were titrated using 1.14mM, 750μM, 500μM of WT UBL domain in the syringe, respectively. UbcH7 and UBL titrations were performed at 20°C in 50mM HEPES pH 7.5, 200mM NaCl, 250μM of TCEP and PBS, 500μM of TCEP, respectively.

Ubiquitination assay

Ubiquitination reactions were performed at 30°C in 50mM Tris pH 7.5, 100mM NaCl, 2.5mM $Mgcl_2$, 5% glycerol, 500μM TCEP. Ubiquitin chain extension reactions contained 25nm of recombinant human E1, 500nM of UbcH7, 1μM E3 and 5mM of ATP in 20 μl of final reaction volume. 0.5 μM of pUB/ WT-UB was used as an allosteric activator in various reactions. Ubiquitination reaction was analysed using 3μM of fluorescently labelled ubiquitin (Ub^{IR800}). Ubiquitin labelling was performed using DyLight™ 800 Maleimide as described before 23. Miro1 ubiquitination was performed in the similar setup using 5μM of Miro1 (181-592) and 12.5nm of recombinant human E1, 250nM of UbcH7, 0.5μM E3 and 5mM of ATP in 20 μl of final reaction volume. For Figure 3d, UBS65A/WT-Ub/ UbcH7C86K/UbcH7C86K~Ub were phosphorylated in separate reactions with GST tagged TcPINK1; UbcH7C86K~Ub with no PINK1 was used as control. Prior to addition to Ubiquitination reaction, PINK1 was depleted using GST resin.

Miro1 ubiquitination was performed in the similar setup using 5μM of Miro1 (181-592) and 12.5nm of recombinant human E1, 250nM of UbcH7, 0.5μM (unless otherwise specified) E3 and 5mM of ATP in 20 μl of final reaction volume. All assays were repeated at least 3 times.

Parkin ubiquitin loading

Reactions monitoring RING2(Rcat)-ubiquitin ester formation were performed at 30°C for 90 min in 50mM Tris pH 7.5, 100mM NaCl, 5mM $MgCl_2$, 1mM TCEP and 0.5% polyethylene glycol 6000 reaction buffer. Reactions contained 50nm E1, 10μM UbcH7, 10μM Ub^{IR800}, 3μM E3 and 5mM ATP in final reaction volume of 10μl. Non-activatable pUb-6His (3μM) was used as an allosteric activator where indicated. Reactions were stopped using NuPAGE LDS Sample Buffer (Invitrogen) that contained reducing agents and boiled for 5min. To hydrolyse ester linkages the boiled samples were cooled and further treated with 0.4M NaOH for 20 min at 42°C. The samples were resolved by SDS-PAGE and analyzed by direct fluorescence monitoring using Li-COR Odyssey Infrared Imaging System. Integrated intensities of Parkin-Ub ester species from three independent experiments were obtained using Image Studio (Odyssey) imaging software, plotted as mean ± standard error of mean (SEM) and statistically analysed using GraphdPad Prism7.

Chemical Shift Perturbations

A complex of $^{2}H,^{12}C,^{15}N$-labelled R0RBR with ^{2}H-labelled pUb (prepared as above) was purified to homogeneity using gel filtration chromatography in 25 mM HEPES, 100 mM NaCl, 0.5 mM TCEP at pH 7.0. Chemical shift perturbation experiments were measured using $^{1}H,^{15}N$-TROSY spectra of 205 μM $^{2}H,^{12}C,^{15}N$-R0RBR/ ^{2}H-pUb in the absence and presence of $^{2}H,^{14}N$-labelled Ub. These experiments were quantified using the following weighted formula: $((0.2 \times \Delta\delta N^{2}) + \Delta\delta H^{2})^{1/2}$ and plotted as a function of residue. All NMR experiments were collected using a triple resonance cryogenic probe on a Varian Inova 600 MHz NMR spectrometer at 25°C.

Supplementary Material

Refer to Web version on PubMed Central for supplementary material.

Acknowledgements

We thank L. Briere for her expertise and help in collecting and analyzing the sedimentation velocity data. This work was supported by the Cancer Research UK [grant number 17739]; the Medical Research Council [grant number MC_UU_12016/12]; and the EMBO Young Investigator Programme (HW). This work was supported by a grant from the Canadian Institutes of Health Research (MOP-14606) and the Canada Research Chairs Program (GSS).

References

1. Bonifati V, et al. Autosomal recessive early onset parkinsonism is linked to three loci: PARK2, PARK6, and PARK7. Neurol Sci. 2002; 23(Suppl 2):S59–60. [PubMed: 12548343]
2. Martin I, Dawson VL, Dawson TM. Recent advances in the genetics of Parkinson's disease. Annu Rev Genomics Hum Genet. 2011; 12:301–25. [PubMed: 21639795]
3. Kitada T, et al. Mutations in the parkin gene cause autosomal recessive juvenile parkinsonism. Nature. 1998; 392:605–8. [PubMed: 9560156]
4. Valente EM, et al. Hereditary early-onset Parkinson's disease caused by mutations in PINK1. Science. 2004; 304:1158–60. [PubMed: 15087508]
5. Chung SY, et al. Parkin and PINK1 Patient iPSC-Derived Midbrain Dopamine Neurons Exhibit Mitochondrial Dysfunction and alpha-Synuclein Accumulation. Stem Cell Reports. 2016; 7:664–677. [PubMed: 27641647]
6. Exner N, Lutz AK, Haass C, Winklhofer KF. Mitochondrial dysfunction in Parkinson's disease: molecular mechanisms and pathophysiological consequences. EMBO J. 2012; 31:3038–62. [PubMed: 22735187]
7. Narendra D, Walker JE, Youle R. Mitochondrial quality control mediated by PINK1 and Parkin: links to parkinsonism. Cold Spring Harb Perspect Biol. 2012; 4
8. Walden H, Martinez-Torres RJ. Regulation of Parkin E3 ubiquitin ligase activity. Cell Mol Life Sci. 2012; 69:3053–67. [PubMed: 22527713]
9. Dawson TM, Dawson VL. The role of parkin in familial and sporadic Parkinson's disease. Mov Disord. 2010; 25(Suppl 1):S32–9. [PubMed: 20187240]
10. Kahle PJ, Haass C. How does parkin ligate ubiquitin to Parkinson's disease? EMBO Rep. 2004; 5:681–5. [PubMed: 15229644]
11. Lim KL, Dawson VL, Dawson TM. Parkin-mediated lysine 63-linked polyubiquitination: a link to protein inclusions formation in Parkinson's and other conformational diseases? Neurobiol Aging. 2006; 27:524–9. [PubMed: 16213628]
12. Spratt DE, Walden H, Shaw GS. RBR E3 ubiquitin ligases: new structures, new insights, new questions. Biochem J. 2014; 458:421–37. [PubMed: 24576094]
13. Spratt DE, et al. A molecular explanation for the recessive nature of parkin-linked Parkinson's disease. Nat Commun. 2013; 4:1983. [PubMed: 23770917]
14. Stieglitz B, et al. Structural basis for ligase-specific conjugation of linear ubiquitin chains by HOIP. Nature. 2013; 503:422–6. [PubMed: 24141947]
15. Lazarou M, et al. PINK1 drives Parkin self-association and HECT-like E3 activity upstream of mitochondrial binding. J Cell Biol. 2013; 200:163–72. [PubMed: 23319602]
16. Riley BE, et al. Structure and function of Parkin E3 ubiquitin ligase reveals aspects of RING and HECT ligases. Nat Commun. 2013; 4:1982. [PubMed: 23770887]
17. Stieglitz B, Morris-Davies AC, Koliopoulos MG, Christodoulou E, Rittinger K. LUBAC synthesizes linear ubiquitin chains via a thioester intermediate. EMBO Rep. 2012; 13:840–6. [PubMed: 22791023]
18. Wenzel DM, Lissounov A, Brzovic PS, Klevit RE. UBCH7 reactivity profile reveals parkin and HHARI to be RING/HECT hybrids. Nature. 2011; 474:105–8. [PubMed: 21532592]
19. Zheng X, Hunter T. Parkin mitochondrial translocation is achieved through a novel catalytic activity coupled mechanism. Cell Res. 2013; 23:886–97. [PubMed: 23670163]
20. Beasley SA, Hristova VA, Shaw GS. Structure of the Parkin in-between-ring domain provides insights for E3-ligase dysfunction in autosomal recessive Parkinson's disease. Proc Natl Acad Sci U S A. 2007; 104:3095–100. [PubMed: 17360614]

21. Hristova VA, Beasley SA, Rylett RJ, Shaw GS. Identification of a novel Zn2+-binding domain in the autosomal recessive juvenile Parkinson-related E3 ligase parkin. J Biol Chem. 2009; 284:14978–86. [PubMed: 19339245]
22. Chaugule VK, et al. Autoregulation of Parkin activity through its ubiquitin-like domain. EMBO J. 2011; 30:2853–67. [PubMed: 21694720]
23. Kumar A, et al. Disruption of the autoinhibited state primes the E3 ligase parkin for activation and catalysis. EMBO J. 2015; 34:2506–21. [PubMed: 26254304]
24. Sauve V, et al. A Ubl/ubiquitin switch in the activation of Parkin. EMBO J. 2015
25. Trempe JF, et al. Structure of parkin reveals mechanisms for ubiquitin ligase activation. Science. 2013; 340:1451–5. [PubMed: 23661642]
26. Wauer T, Komander D. Structure of the human Parkin ligase domain in an autoinhibited state. EMBO J. 2013; 32:2099–112. [PubMed: 23727886]
27. Kane LA, et al. PINK1 phosphorylates ubiquitin to activate Parkin E3 ubiquitin ligase activity. J Cell Biol. 2014; 205:143–53. [PubMed: 24751536]
28. Kazlauskaite A, et al. Parkin is activated by PINK1-dependent phosphorylation of ubiquitin at Ser65. Biochem J. 2014; 460:127–39. [PubMed: 24660806]
29. Kondapalli C, et al. PINK1 is activated by mitochondrial membrane potential depolarization and stimulates Parkin E3 ligase activity by phosphorylating Serine 65. Open Biol. 2012; 2:120080. [PubMed: 22724072]
30. Koyano F, et al. Ubiquitin is phosphorylated by PINK1 to activate parkin. Nature. 2014; 510:162–6. [PubMed: 24784582]
31. Okatsu K, et al. PINK1 autophosphorylation upon membrane potential dissipation is essential for Parkin recruitment to damaged mitochondria. Nat Commun. 2012; 3:1016. [PubMed: 22910362]
32. Shiba-Fukushima K, et al. PINK1-mediated phosphorylation of the Parkin ubiquitin-like domain primes mitochondrial translocation of Parkin and regulates mitophagy. Sci Rep. 2012; 2:1002. [PubMed: 23256036]
33. Kirisako T, et al. A ubiquitin ligase complex assembles linear polyubiquitin chains. EMBO J. 2006; 25:4877–87. [PubMed: 17006537]
34. Moynihan TP, et al. The ubiquitin-conjugating enzymes UbcH7 and UbcH8 interact with RING finger/IBR motif-containing domains of HHARI and H7-AP1. J Biol Chem. 1999; 274:30963–8. [PubMed: 10521492]
35. Smit JJ, et al. The E3 ligase HOIP specifies linear ubiquitin chain assembly through its RING-IBR-RING domain and the unique LDD extension. EMBO J. 2012; 31:3833–44. [PubMed: 22863777]
36. Tokunaga F, et al. SHARPIN is a component of the NF-kappaB-activating linear ubiquitin chain assembly complex. Nature. 2011; 471:633–6. [PubMed: 21455180]
37. Duda DM, et al. Structure of HHARI, a RING-IBR-RING ubiquitin ligase: autoinhibition of an Ariadne-family E3 and insights into ligation mechanism. Structure. 2013; 21:1030–41. [PubMed: 23707686]
38. Kelsall IR, et al. TRIAD1 and HHARI bind to and are activated by distinct neddylated Cullin-RING ligase complexes. EMBO J. 2013; 32:2848–60. [PubMed: 24076655]
39. Scott DC, et al. Two Distinct Types of E3 Ligases Work in Unison to Regulate Substrate Ubiquitylation. Cell. 2016; 166:1198–1214 e24. [PubMed: 27565346]
40. Caulfield TR, Fiesel FC, Springer W. Activation of the E3 ubiquitin ligase Parkin. Biochem Soc Trans. 2015; 43:269–74. [PubMed: 25849928]
41. Ham SJ, et al. Interaction between RING1 (R1) and the Ubiquitin-like (UBL) Domains Is Critical for the Regulation of Parkin Activity. J Biol Chem. 2016; 291:1803–16. [PubMed: 26631732]
42. Kazlauskaite A, et al. Binding to serine 65-phosphorylated ubiquitin primes Parkin for optimal PINK1-dependent phosphorylation and activation. EMBO Rep. 2015; 16:939–54. [PubMed: 26116755]
43. Wauer T, Simicek M, Schubert A, Komander D. Mechanism of phospho-ubiquitin-induced PARKIN activation. Nature. 2015; 524:370–4. [PubMed: 26161729]
44. Lechtenberg BC, et al. Structure of a HOIP/E2~ubiquitin complex reveals RBR E3 ligase mechanism and regulation. Nature. 2016; 529:546–50. [PubMed: 26789245]

45. Dove KK, Stieglitz B, Duncan ED, Rittinger K, Klevit RE. Molecular insights into RBR E3 ligase ubiquitin transfer mechanisms. EMBO Rep. 2016; 17:1221–35. [PubMed: 27312108]
46. Aguirre JD, Dunkerley KM, Mercier P, Shaw GS. Structure of phosphorylated UBL domain and insights into PINK1-orchestrated parkin activation. Proc Natl Acad Sci U S A. 2017; 114:298–303. [PubMed: 28007983]
47. Caulfield TR, et al. Phosphorylation by PINK1 releases the UBL domain and initializes the conformational opening of the E3 ubiquitin ligase Parkin. PLoS Comput Biol. 2014; 10:e1003935. [PubMed: 25375667]
48. Im E, Yoo L, Hyun M, Shin WH, Chung KC. Covalent ISG15 conjugation positively regulates the ubiquitin E3 ligase activity of parkin. Open Biol. 2016; 6
49. Ordureau A, et al. Defining roles of PARKIN and ubiquitin phosphorylation by PINK1 in mitochondrial quality control using a ubiquitin replacement strategy. Proc Natl Acad Sci U S A. 2015; 112:6637–42. [PubMed: 25969509]
50. Wauer T, et al. Ubiquitin Ser65 phosphorylation affects ubiquitin structure, chain assembly and hydrolysis. EMBO J. 2015; 34:307–25. [PubMed: 25527291]
51. Tokunaga F, et al. Involvement of linear polyubiquitylation of NEMO in NF-kappaB activation. Nat Cell Biol. 2009; 11:123–32. [PubMed: 19136968]
52. Lazarou M, et al. The ubiquitin kinase PINK1 recruits autophagy receptors to induce mitophagy. Nature. 2015; 524:309–14. [PubMed: 26266977]
53. Ordureau A, et al. Quantitative proteomics reveal a feedforward mechanism for mitochondrial PARKIN translocation and ubiquitin chain synthesis. Mol Cell. 2014; 56:360–75. [PubMed: 25284222]
54. Muller-Rischart AK, et al. The E3 ligase parkin maintains mitochondrial integrity by increasing linear ubiquitination of NEMO. Mol Cell. 2013; 49:908–21. [PubMed: 23453807]
55. Ardley HC, Tan NG, Rose SA, Markham AF, Robinson PA. Features of the parkin/ariadne-like ubiquitin ligase, HHARI, that regulate its interaction with the ubiquitin-conjugating enzyme, Ubch7. J Biol Chem. 2001; 276:19640–7. [PubMed: 11278816]
56. Wright JD, Mace PD, Day CL. Noncovalent Ubiquitin Interactions Regulate the Catalytic Activity of Ubiquitin Writers. Trends Biochem Sci. 2016; 41:924–937. [PubMed: 27614784]
57. Woodroof HI, et al. Discovery of catalytically active orthologues of the Parkinson's disease kinase PINK1: analysis of substrate specificity and impact of mutations. Open Biol. 2011; 1:110012. [PubMed: 22645651]
58. Abdul Rehman SA, et al. MINDY-1 Is a Member of an Evolutionarily Conserved and Structurally Distinct New Family of Deubiquitinating Enzymes. Mol Cell. 2016; 63:146–55. [PubMed: 27292798]
59. Borodovsky A, et al. Chemistry-based functional proteomics reveals novel members of the deubiquitinating enzyme family. Chem Biol. 2002; 9:1149–59. [PubMed: 12401499]
60. Collaborative Computational Project N. The CCP4 suite: programs for protein crystallography. Acta Crystallogr D Biol Crystallogr. 1994; 50:760–3. [PubMed: 15299374]
61. Emsley P, Cowtan K. Coot: model-building tools for molecular graphics. Acta Crystallogr D Biol Crystallogr. 2004; 60:2126–32. [PubMed: 15572765]
62. Bricogne, G., et al. BUSTER 2.11.2. Cambridge, UK: Global Phasing Ltd; 2011.
63. Chen VB, et al. MolProbity: all-atom structure validation for macromolecular crystallography. Acta Crystallogr D Biol Crystallogr. 2010; 66:12–21. [PubMed: 20057044]

Europe PMC Funders Author Manuscripts

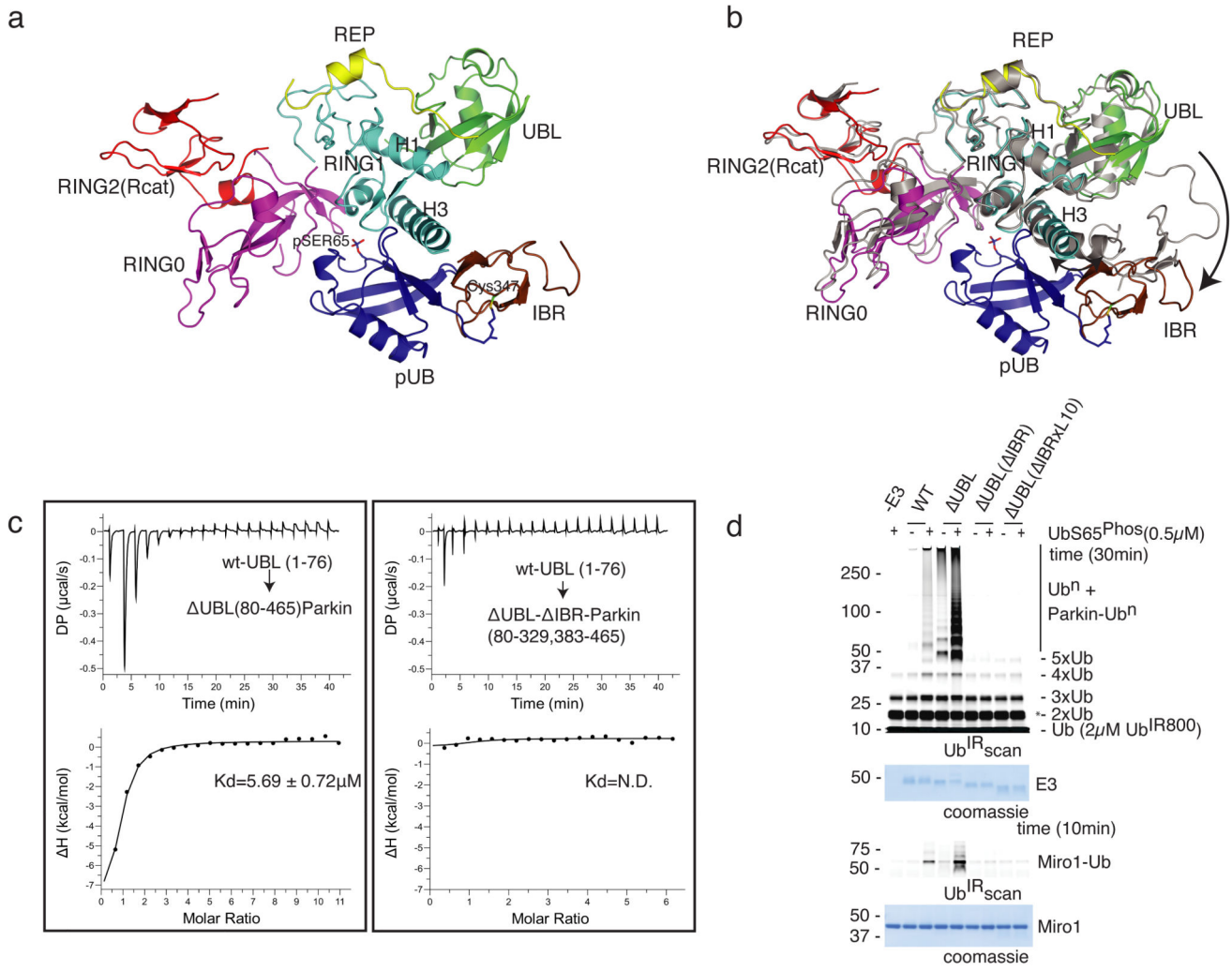

Figure 1. Overall structure of Parkin-phosphoubiquitin complex in the activated state

a) Crystal structure of UBLR0RBR and pUb complex showing UBL, RING0, RING1, IBR, REP, and RING2(Rcat) of Parkin, in complex with phosphoubiquitin (blue). The phosphate group of phosphoubiquitin is shown in stick representation.

b) Comparison of UBLR0RBR-pUb complex (coloured) with the apo structure of UBLR0RBR (grey) (PDB code 5C1Z 23). UBLR0RBR superimposed on the UBLR0RBR-pUb complex structure shows conformational changes between the IBR and the UBL domain, and the void formed (marked with arrow), helix 1 (H1) and helix 3 (H3) of RING1 are marked. UBL (green) remains associated with H1 of RING1 (cyan) in both apo and complex structures.

c) Isothermal Titration Calorimetry assays showing UBL interaction with ΔUBL Parkin (left panel), and that deletion of IBR in ΔUBL Parkin leads to loss of UBL and Parkin interaction (right panel).

d) Deletion of the IBR in ΔUBL Parkin leads to loss of E3 ligase activity of Parkin in ubiquitin chain formation, Parkin autoubiquitination, and Miro1 ubiquitination. FL (autoinhibited) or ΔUBL (active) Parkin comparison is shown with ΔUBL-ΔIBR Parkin, or

ΔUBL-ΔIBR with a 10-residue linker in the presence or absence of pUb. Uncropped gel images are shown in Supplementary Data Set 1.

Europe PMC Funders Author Manuscripts

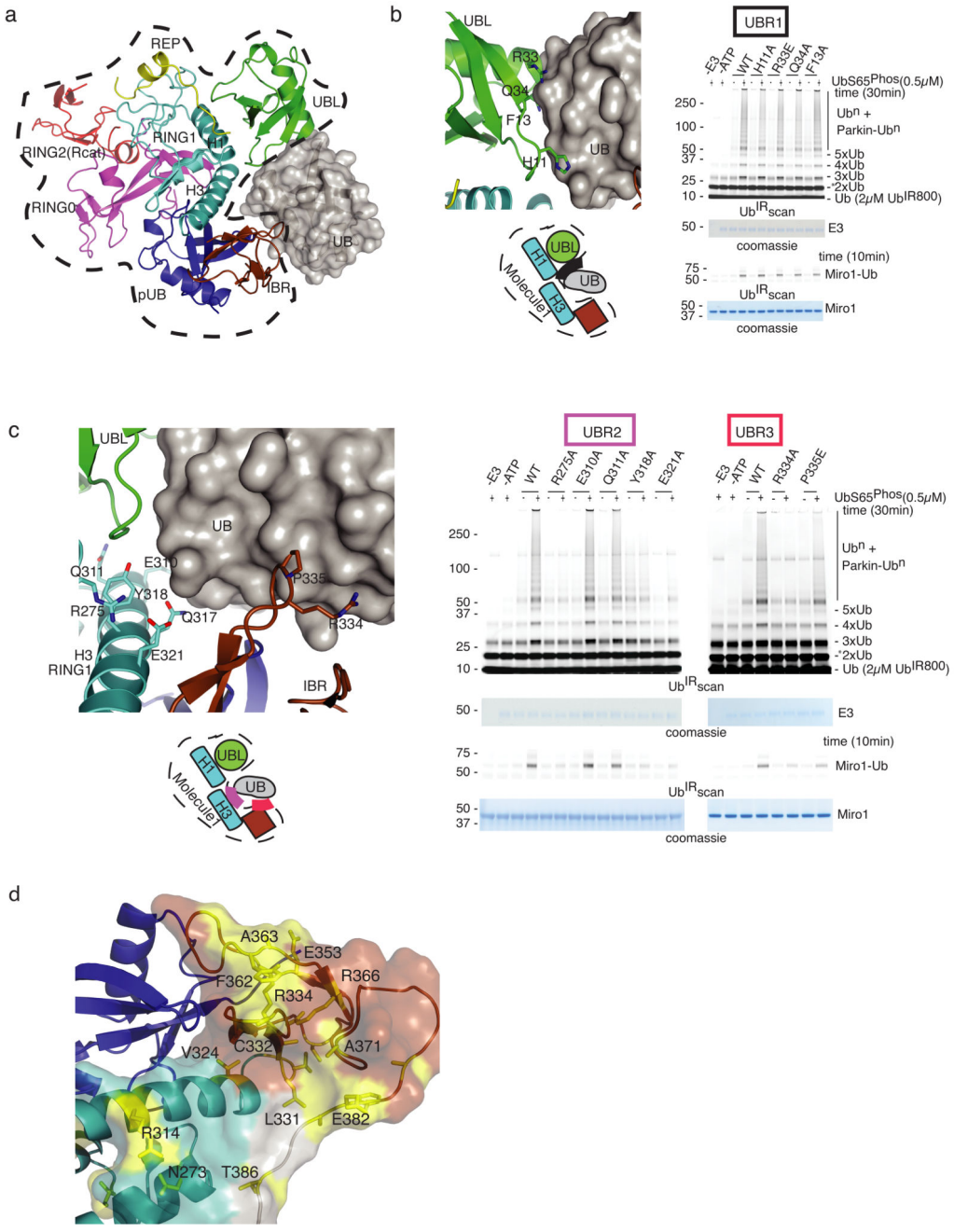

Figure 2. Identification of potential ubiquitin binding regions important for Parkin function.

a) Model of ubiquitin (grey surface) binding to Parkin, based on crystallographic packing of a second Parkin molecule (shown in Supp Fig 2b). The boundary of one UBLR0RBR-pUb complex (domains coloured as in Figure 1) is represented by a dashed line.

b) The UBL (green) and forms ubiquitin binding region 1 (UBR1) (left panel). For clarity, UBL (green), modelled ubiquitin (grey), RING1 helices H1, H3 (cyan), IBR (brown) are schematically represented below, with molecule 1 boundary of Parkin marked with a dashed line, and UBR1 marked as a shaded box. The activity of UBR1 mutants was monitored by

Europe PMC Funders Author Manuscripts

Europe PMC Funders Author Manuscripts

fluorescently-labelled ubiquitin incorporation into ubiquitin chains and Parkin autoubiquitination, and Miro1 ubiquitination (right panel). Coomassie-stained gel is shown as loading control. In this and in all subsequent ubiquitination assays, a non-specific, ATP-independent band is indicated (*).

c) H3 of RING1 (cyan) and IBR (brown) make 2 important interfaces with ubiquitin (grey) (left upper panel), shown as UBR2 (purple box) and UBR3 (red box), respectively (left lower panel). Mutations in UBR2 and UBR3 of Parkin lead to loss of E3 ligase activity of Parkin in ubiquitin chain formation, Parkin autoubiquitination, and Miro1 ubiquitination (right panel). Assay conditions are as in panel b.

d) Chemical shift perturbation map obtained from NMR titration experiments where $^{2}H,^{14}N$-labelled Ub was titrated into a solution of $^{2}H,^{12}C,^{15}N$-labelled R0RBR Parkin in complex with ^{2}H-labelled pUb, and followed by $^{1}H,^{15}N$ TROSY experiments. Residues that experienced chemical shift changes greater than 1 standard deviation above the average shift in the absence of Ub are indicated in yellow.

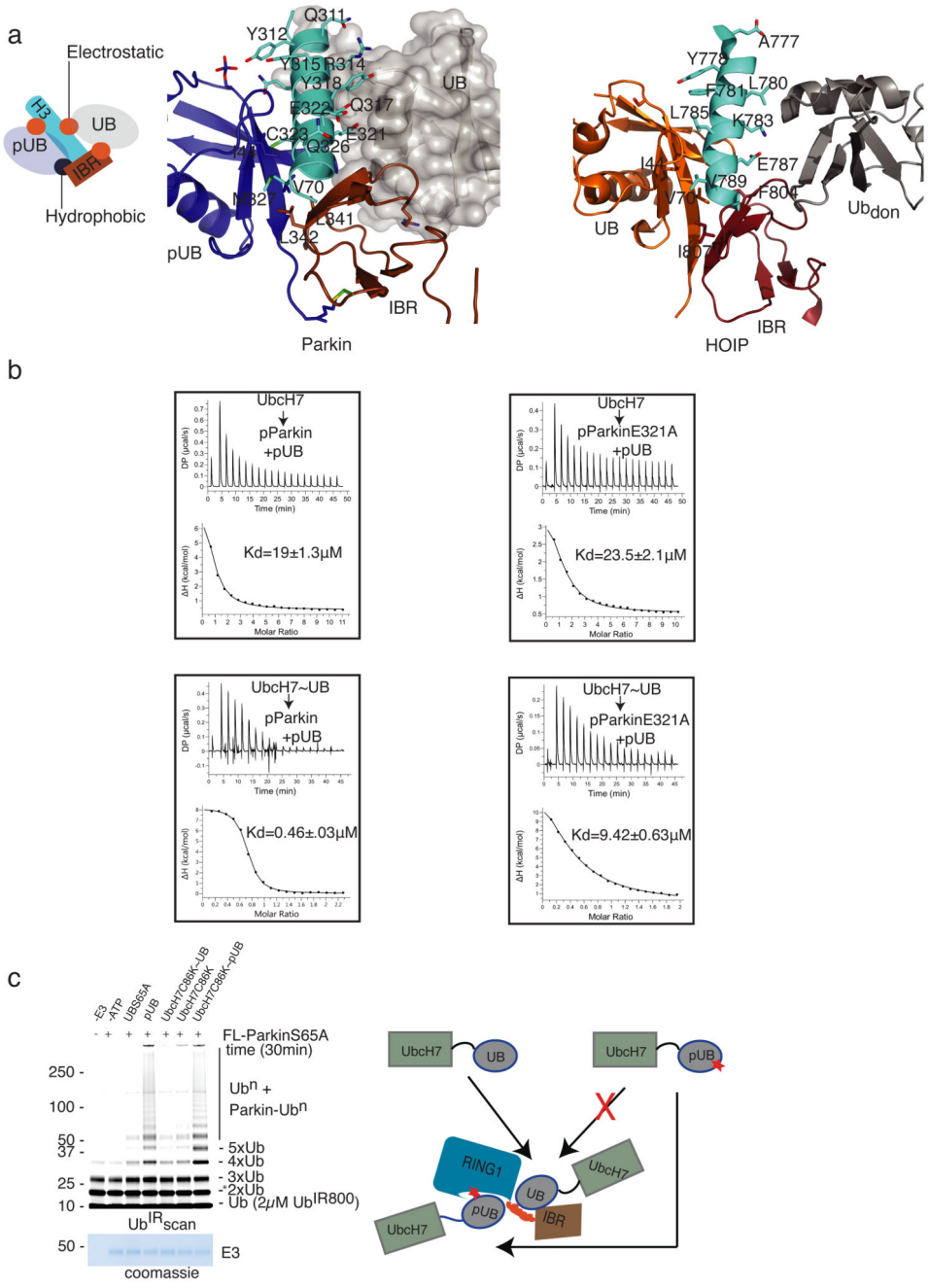

Figure 3. Parkin activation promotes donor ubiquitin (Ub_{don}) binding at H3-IBR interface

a) Nature of interactions (red sphere: electrostatic, black sphere: hydrophobic) between pUb (blue)/UB (grey) and H3 (cyan)/IBR (brown) of Parkin are shown schematically (left panel). Residues on H3 (cyan)-IBR (brown) of Parkin interacting with pUb (blue) and Ub (grey surface) (modelled by superposition on UBL of molecule 2 in the UBLR0RBR-pUb complex structure) are shown as sticks (middle panel). Helix-connecting-RING1-IBR and IBR of HOIP interaction with activator ubiquitin (Ub) and donor ubiquitin (Ub_{don}) (pdb code 5EDV 44).

b) Isothermal Titration Calorimetry assays showing Glu321Ala mutation does not affect Parkin interaction with UbcH7 (upper panel), but does reduce Parkin interaction with the UbcH7~Ub iso-peptide (lower panel). ITC measurements were performed using phosphorylated Parkin in the presence of pUb.

c) Parkin can be activated by UbcH7C86K~pUb conjugate similarly to pUb. Ubiquitination assay was performed with 1μM of ParkinS65A. Parkin was activated with 1μM of UbS65A/pUb/UbcH7C86K~Ub/UbcH7C86K/UbcH7C86K~pUb (Left panel), coomassie-stained gel is shown as loading control (lower panel). A model depicting distinct ubiquitin (UbcH7~Ub or pUb/UbcH7C86K~pUB) binding regions on Parkin is shown in the right panel.

Europe PMC Funders Author Manuscripts

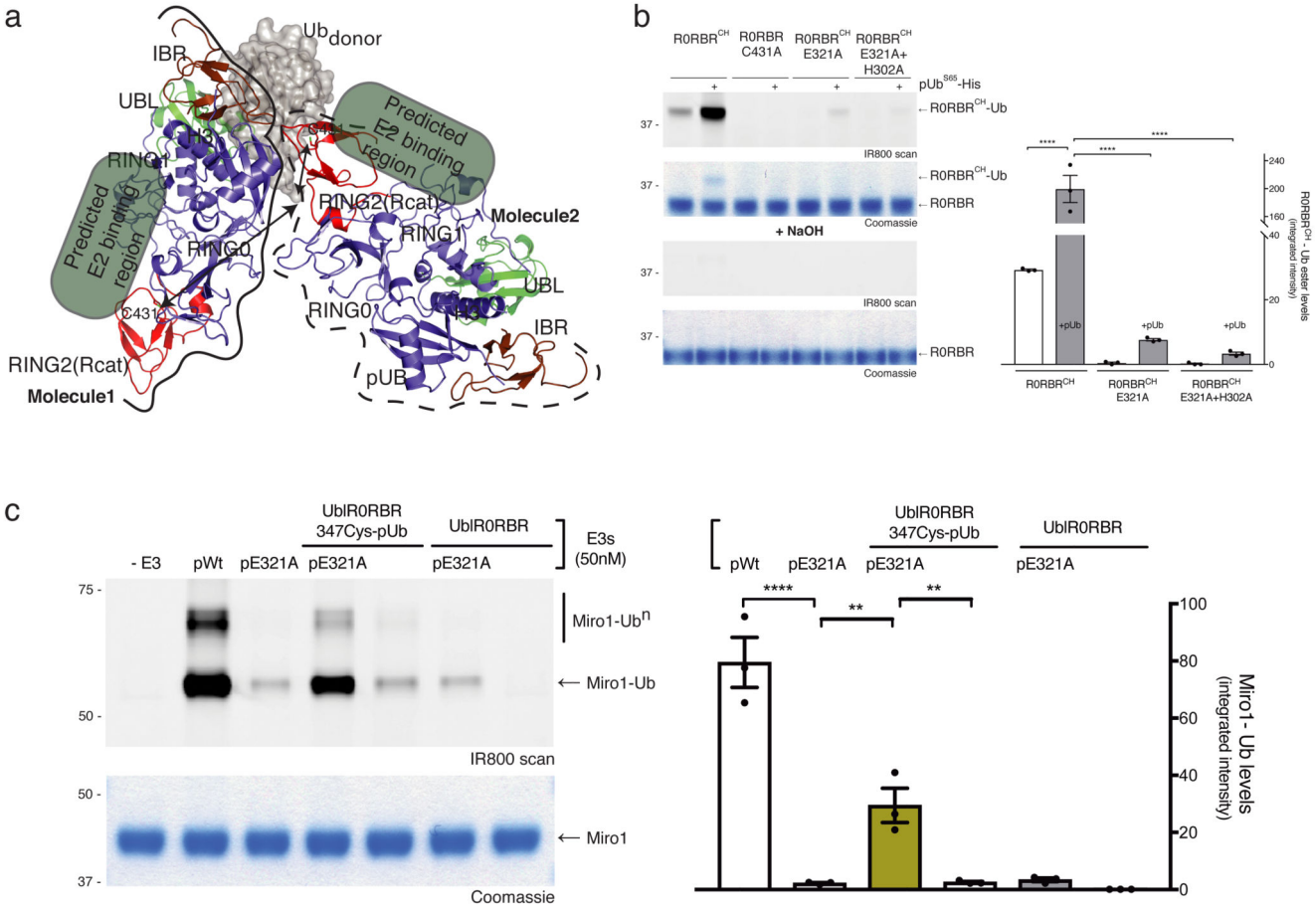

Figure 4. Parkin molecules cooperate to facilitate ubiquitin transfer

a) Model of crystal packing between molecules of Parkin. The modelled donor ubiquitin (grey surface) sits above the catalytic cysteine (C431) of the RING2(Rcat) (red) of a neighbouring Parkin molecule. For clarity, the rest of the Parkin molecules are shown in slate, except for the UBL domain (green), and IBR (brown). The predicted E2 binding region on each molecule is shown.

b) Mutation of UBR2 and phosphoubiquitin patches of Parkin leads to defects in formation of a RING2(Rcat)-Ub ester intermediate, monitored using fluorescently-labelled ubiquitin (left top). Sodium hydroxide sensitivity confirms the RING2(Rcat)-ubiquitin ester bond (left bottom). Coomassie-stained gels are shown as total Parkin levels. Integrated intensities of Parkin-Ub ester levels from three independent experiments were plotted as mean ± SEM (right). Statistical significance was determined by one-way analysis of variance with Bonferroni's multiple-comparison test. (n = 3, ****P < 0.0001).

c) Activated UblR0RBR complexed with phosphoubiquitin can stimulate the activity of inactive Parkin. The activity of phosphoParkin mutated in the ubiquitin donor binding site (E321A) is enhanced by the addition of UblR0RBR Parkin covalently complexed with phosphoubiquitin. Addition of UblR0RBR Parkin alone does not enhance the activity of pParkinE321A. Ubiquitination of Miro1 is monitored using fluorescently-labelled ubiquitin (left top). Coomassie stained gel shows total Miro1 levels (left bottom). Integrated intensities

Europe PMC Funders Author Manuscripts

of Miro1-Ub levels from three independent experiments were plotted as mean ± SEM (right). Statistical significance was determined by one-way analysis of variance with Bonferroni's multiple-comparison test. (n = 3, ****P < 0.0001, **P < 0.01)

Europe PMC Funders Author Manuscripts

Europe PMC Funders Author Manuscripts

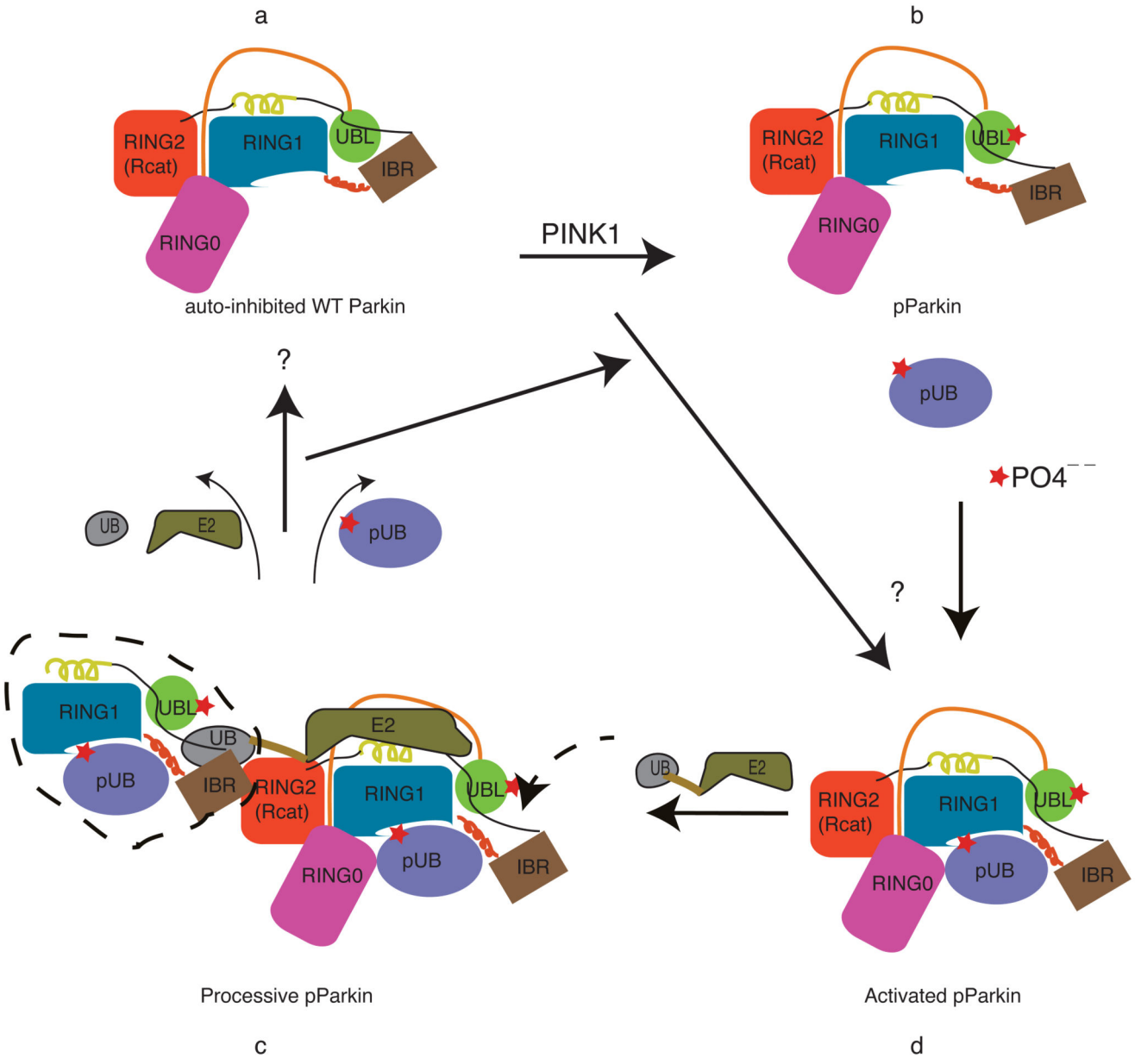

Figure 5. Model of Parkin regulation

a) Parkin is autoinhibited by UBL blocking IBR (brown) and H3 (red) of RING1 (cyan).

b) Phosphorylation (marked with red asterisk) of UBL/pUb binding creates a pocket at H3-IBR and UBL interface, leading to activated Parkin.

c) Activated Parkin shows small rearrangements triggered by the straightening of the H3-IBR helix. Loaded E2 (E2~Ub) is recognised at this new interface, E2 occupying interface with REP and RING1 of activated Parkin, Ub_{don} (grey) sitting on the interface of IBR (brown box) and H3 (red helix) of RING1 of neighbouring molecule of Parkin (marked with a dashed line).

Europe PMC Funders Author Manuscripts

Table 1
Data collection and refinement statistics (molecular replacement)

	UBLR0RBR+pUb (5N2W)	S65DUBLR0RBR+pUb (5N38)
Data collection		
Space group	P63 2 2	P63 2 2
Cell dimensions		
a, *b*, *c* (Å)	147.3 147.3 87.5	146.5 146.5 88.4
α, *β*, *γ*(°)	90 90 120	90 90 120
Resolution (Å)	56.34-2.68 (2.81-2.68)[a]	72.56-2.60 (2.76-2.60)[a]
R_{merge}	10.7 (71.9)	8.2 (48.4)
$I/\sigma(I)$	8.9 (1.9)	9.1 (2.2)
$CC_{1/2}$	99.4 (66.8)	99.5 (64.0)
Completeness (%)	93.6 (93.7)	96.4 (88.4)
Redundancy	4.6 (4.2)	3.5 (3.2)
Refinement		
Resolution (Å)	56.34 (2.68)	72.56 (2.60)
No. reflections	15007	16984
R_{work} / R_{free}	19.93/24.17	18.16/22.86
No. atoms		
Protein	3619	3565
Ligand/ion	23[a]	17[b]
Water	29	46
B factors		
Protein	60.2	55.9
Ligand/ion	84.4	79.1
Water	53.4	37.8
R.m.s. deviations		
Bond lengths (Å)	0.01	0.01
Bond angles (°)	1.14	1.17

Single crystals were used for structure determination.

[a] 8 Zinc ions, 1 Chloride ion, 10 trimethyloxide atoms, 4 aminopropane atoms

[b] 8 Zinc ions, 1 Chloride ion, 4 polyethylene glycol atoms, 4 aminopropane atoms